Polymer 49 (2008) 3176–3185

Contents lists available at ScienceDirect

Polymer

journal homepage: www.elsevier.com/locate/polymer

Structural relaxation of polyvinyl acetate (PVAc)

Roman Svoboda [a,*], Pavla Pustková [b], Jiří Málek [a]

[a] Department of Physical Chemistry, Faculty of Chemical Technology, University of Pardubice, Cs. Legii 565, 532 10 Pardubice, Czech Republic
[b] Department of Inorganic Technology, Faculty of Chemical Technology, University of Pardubice, Cs. Legii 565, 532 10 Pardubice, Czech Republic

ARTICLE INFO

Article history:
Received 4 March 2008
Received in revised form 25 April 2008
Accepted 1 May 2008
Available online 8 May 2008

Keywords:
Polyvinyl acetate
Glass transition
Structural relaxation

ABSTRACT

Structural relaxation of polyvinyl acetate (PVAc) was studied by mercury dilatometry and differential scanning calorimetry. Tool–Narayanaswamy–Moynihan (TNM) and Adam–Gibbs–Scherer (AGS) models were used to fit numerous experimental data. Single set of volume and enthalpy relaxation parameters describing all performed experiments was found for each model. Comparison of volume and enthalpy relaxation was made on the basis of TNM parameter values. The famous volume relaxation measurements made by Kovacs [Fortschr Hochpolym Forsch 1963;3:394–507] were successfully fitted using the same set of parameters. Furthermore, several non-fitting methods of TNM parameters' estimation (including, e.g., peak-shift method or inflectional analysis) were applied to our data and their critical comparison is outlined. For most methods a good agreement with curve-fitting results was achieved.

1. Introduction

Glass transition is a widely studied phenomenon that can be shortly described as a process at which some macroscopic property (volume, enthalpy, refraction index…) departs during continuing cooling from the undercooled liquid equilibrium state. The slope of the property–temperature curve decreases from its undercooled liquid value (higher temperature) to the glassy value (lower temperature). At that moment the glass is formed and the glass transition temperature T_g can be evaluated as an intersection of the liquid and glassy asymptotes. Glass transition temperature is cooling rate dependent as the system departs from equilibrium due to the timescale for molecular motions becoming longer than the time available for these motions (which is determined by the cooling rate) [1]. In other words, at T_g the system can no longer achieve its structural equilibrium within the available time given by the rate of cooling. The non-equilibrium nature of the glassy state results in structural relaxation. This process often called "physical aging" occurs within and below the glass transition region and can be described as the spontaneous change of the structure towards its equilibrium state represented by the undercooled liquid extrapolation to the given temperature (Fig. 1). The rate at which the system approaches the equilibrium depends on actual temperature and structure (i.e. thermal history) of the glass [2]. Structural relaxation is often classified according to the property that is being observed – e.g. the volume or enthalpy relaxation.

Structural relaxation has been intensively studied in polymers during past decades and many excellent reviews were written [1–5]. Polyvinyl acetate was often chosen as a model low-molecular polymer for structural relaxation studies. Pioneering work on the field of structural relaxation was probably that of Kovacs, who made an extensive study of the volume relaxation in glassy polymers [6]. His PVAc volume relaxation data measured using mercury

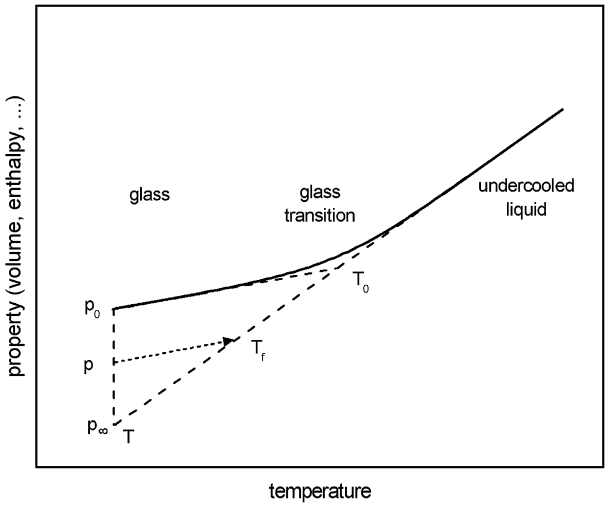

Fig. 1. Temperature dependence of a property (volume or enthalpy) relaxing at constant pressure. Index "0" represents initial state of the formed glass while index "∞" represents the equilibrium state of the material. Evaluation of the fictive temperature T_f is demonstrated.

* Corresponding author. Tel.: +420 466 037 045.
E-mail address: roman.svoboda@atlas.cz (R. Svoboda).

0032-3861/$ – see front matter © 2008 Elsevier Ltd. All rights reserved.
doi:10.1016/j.polymer.2008.05.002

dilatometry are apparently the most famous ones and are discussed and tested by newly developed models till nowadays [7–10]. Besides this work, volume relaxation of PVAc by the use of mercury dilatometry was studied by Delin et al. [11] or Cowie et al. [12], and *P–V–T* glass formation data for polyvinyl acetate were published by McKinney and Goldstein [13]. Enthalpy relaxation measurements of polyvinyl acetate were performed, e.g., by Hutchinson and Kumar [14], Sasabe and Moynihan [15] or Hodge [16]. The comparison of different types of structural relaxation is one of the main intentions of contemporary authors publishing on the discussed field [11,12,17–19].

In the present paper, the volume and enthalpy relaxation of polyvinyl acetate have been investigated using mercury dilatometry and differential scanning calorimetry. The objectives of this work are: (1) to describe and compare both volume and enthalpy data by evaluating the parameters of TNM (Tool–Narayanaswamy–Moynihan) and AGS (Adam–Gibbs–Scherer) models using the curve-fitting method; (2) to compare several non-fitting methods of evaluating the TNM parameters with the curve-fitting results.

2. Theory

2.1. TNM and AGS models

It is a well-known fact that structural relaxation is the non-exponential and non-linear process. Non-exponentiality of the structural relaxation is often described by means of the distribution of relaxation times which is expressed by the Kohlrausch–Williams–Watts (KWW) stretched exponential function [20,21]. The KWW function is defined as follows:

$$\Phi(t) = \exp\left(-\xi^{\beta}\right) = \exp\left[-\left(\int_0^t \frac{\mathrm{d}t}{\tau}\right)^{\beta}\right] \tag{1}$$

where $\Phi(t)$ is the relaxation function, ξ is the reduced time, τ is the relaxation time, which is a function of the temperature T and actual structure of the material, and β is the parameter of non-exponentiality and is inversely related to the width of the relaxation time distribution ($0 \le \beta \le 1$).

The non-linear character of the structural relaxation is often described on the basis of Tool's concept [22] that the relaxation time depends on both temperature and actual structure of the material. This instantaneous structure of the system can be described by the fictive temperature T_f introduced by Tool. The fictive temperature is defined as the temperature of the undercooled liquid which has the same structure as the relaxing glass (Fig. 1). The concept of Tool was then modified by Narayanaswamy and Moynihan [23,24]:

$$\tau(T, T_f) = A_{TNM} \exp\left[\frac{x\,\Delta h^*}{RT} + \frac{(1-x)\Delta h^*}{RT_f}\right] \tag{2}$$

where A_{TNM} is the pre-exponential factor (which stands for the relaxation time at an infinitely high temperature), x is the parameter of non-linearity which describes the temperature/structure ratio of contribution to the relaxation time, $\Delta h^*/R$ is the apparent activation energy of structural relaxation, and the meaning of other symbols is obvious or explained above. The set of Eqs. (1) and (2) became known as the TNM (Tool–Narayanaswamy–Moynihan) model.

Another expression for the non-linearity of structural relaxation was presented by Scherer [25,26] who applied the Adam–Gibbs theory into the formulation of relaxation time. This concept was further improved by Hodge [27] and together with Eq. (1) is known as the AGS (Adam–Gibbs–Scherer) model:

$$\tau(T, T_f) = A_{AGS} \exp\left[\frac{B}{T(1-(T_2/T_f))}\right] \tag{3}$$

where A_{AGS} is the pre-exponential factor with similar meaning as the one in the TNM model described above, B is a constant and T_2 represents the temperature at which the configurational entropy of the liquid would vanish. The temperature T_2 was found to be practically identical with the Kauzmann temperature T_K for some polymers [28].

Evaluation of the TNM and AGS parameters can be done either by the curve-fitting method or with the use of some non-fitting method based on the simple data analysis. Certain frequently used non-fitting methods are presented in the following text.

2.2. Dependence of T_g on cooling rate

An equation derived by Ritland [29] for the relation of the cooling rate and fictive temperature for glasses without memory effects was later extended by Moynihan et al. [24] to systems that exhibit a spectrum of relaxation times. Assuming the concept of thermorheological simplicity, i.e. that the distribution of relaxation times is temperature independent, the fictive temperature T_f, obtained when a glass is cooled through the glass transition region, is shown [24] to be related to the cooling rate q^- by:

$$\frac{\mathrm{d}\ln|q^-|}{\mathrm{d}(1/T_f)} = -\frac{\Delta h^*}{R} \tag{4}$$

where the fictive temperature T_f corresponds to the conventional T_g value obtained on cooling, i.e. to the temperature of intersection of the extrapolated liquid and glass property–temperature curves. Evaluation of the apparent activation energy $\Delta h^*/R$ according to Eq. (4) can easily be performed from the set of three-step DSC measurements. In such measurements, first some short annealing at temperature well above T_g is applied to ensure that the sample is in thermal and structural equilibrium. Then the sample is cooled at a defined cooling rate q^- to some temperature well below T_g for the glass to be fully formed. After the sample is cooled, immediate heating at q^+ to some temperature above T_g is applied. The previous thermal history is displayed during this heating scan in the endothermic peak at T_g (the so-called overshoot). The structure of the glass achieved during the cooling step (represented by T_f) can be evaluated using the "equal area method" [24,30]. This method is based on the following equation:

$$\int_{T^*}^{T_f} (C_{pl} - C_{pg})\mathrm{d}T_f = \int_{T^*}^{T'} (C_p - C_{pg})\mathrm{d}T \tag{5}$$

where T^* is any temperature above T_g at which the heat capacity is equal to the equilibrium undercooled liquid value C_{pl} and T' is a temperature well below T_g where a constant glassy value of C_{pg} was achieved. In order to evaluate $\Delta h^*/R$ from three-step measurements, various cooling rates together with constant heating rate have to be applied.

The same three-step cycles as described above can be used to estimate the non-exponentiality parameter β and/or non-linearity parameter x. [31] If the heating scan curves are normalized in order for C_p to rise from zero (glassy state) to unity (undercooled liquid state) then the C_p value of the maximum of the endothermic peak is denoted by C_p^{max}. The comparison of experimental values of C_p^{max} determined for the set of cooling rates with theoretically modeled values for various combinations of β and x.

2.3. Peak-shift method

The peak-shift method [32,33] is a non-fitting method that provides an estimation of the non-linearity parameter x. This method was originally based on the Kovacs–Aklonis–Hutchinson–Ramos (KAHR) phenomenological model [34] for description of the structural relaxation. In this model the apparent activation energy was related to the temperature factor θ through the following equation:

$$\theta \approx \frac{\Delta h^*}{RT_g^2} \tag{6}$$

Four-step thermal cycles are used in the peak-shift method. First step is a short annealing at temperature well above T_g in order that the sample achieves thermal and structural equilibrium. The equilibrium annealing is followed by a cooling step at constant rate q^- to a temperature T below T_g where annealing for various periods of time t_a is applied. During this annealing the sample relaxes and changes its structure (fictive temperature) towards the equilibrium one. After a certain period of time the sample is immediately heated at a constant heating rate q^+ until equilibrium is established again at high temperature. The amount of relaxation proceeded during the previous annealing step is displayed during the heating scan as the overshoot effect at T_g. To quantify the degree of relaxation during annealing at T the total excess enthalpy δ_H can be evaluated as:

$$\delta_H = \Delta H - \Delta H_0 \tag{7}$$

where ΔH_0 is the equilibrium enthalpy achieved during the cycle with $t_a = 0$ and ΔH stands in this equation for the excess enthalpy achieved during the cycle when relaxation proceeded. Hutchinson and Ruddy [32,33] show that the maximum of the endothermic peak T_p displayed during the heating scan at T_g depends on experimental variables according to the following equations:

$$s(Q^-) = \theta\left(\frac{\partial T_p}{\partial \ln|q^-|}\right)_{\delta_H, q^+} \tag{8}$$

$$s(D_H) = \Delta C_p\left(\frac{\partial T_p}{\partial \delta_H}\right)_{q^-, q^+} \tag{9}$$

$$s(Q^+) = \theta\left(\frac{\partial T_p}{\partial \ln|q^+|}\right)_{\delta_H, q^-} \tag{10}$$

where $s()$ stands for the peak shift of certain property, and Q^-, D_H and Q^+ are the normalized dimensionless variables where $Q^- = \theta q^-$, $D_H = \theta\delta_H/\Delta C_p$ and $Q^+ = \theta q^+$. These shifts were evaluated in limiting conditions of a well-stabilized glass, i.e. of a glass that was annealed for a long time. The importance of this last statement lies in occurrence of the so-called "upper peak" [31] instead of the main annealing peak during the heating scan in the case of poorly stabilized glass (shorter annealing times). The difference in-between these two types of peaks dwells in their dependence on experimental conditions as the temperature of the maximum of the upper peak T_u is almost independent of the amount of annealing δ_H. It was shown [35] for the main annealing peak that the shifts are inter-related:

$$F(x) = s(D_H) = s(Q_2) - 1 = -s(Q_1) \tag{11}$$

The dependence of $F(x)$ on x can be expressed by the following equation:

$$F(x) = x^{-1} - 1 \tag{12}$$

It can be also shown by theoretical simulations that the function $F(x)$ is markedly insensitive to the selection of relaxation time distribution. In practice, the $F(x)$ function is evaluated from $\hat{s}(D_H)$, i.e. from the experimentally determined dependence of T_p on δ_H.

It was further shown [31] from theories outlined above that the apparent activation energy of structural relaxation $\Delta h^*/R$ can be evaluated from three-step DSC experiments where the ratio of the cooling and heating rates remains the same (i.e. the heating rate is not constant as it was in similar experiments mentioned in Section 2.3 but changes together with cooling rate). The evaluation can be performed according to the following equation:

$$-\frac{\Delta h^*}{R} = \left[\frac{\mathrm{d}\ln|q^+|}{\mathrm{d}(1/T_p)}\right]_{q^-/q^+ = \text{constant}} \tag{13}$$

where T_p is the temperature of the maximum of the endothermic relaxation peak.

2.4. Inflectional analysis

Málek [36,37] performed complex data analysis for isothermal down-jump relaxation experiments. The analysis is based on TNM equations, and simulations of down-jump experiments under various conditions showed that TNM parameters can be evaluated from the dependence of the so-called "stabilization period" of the relaxation process on ΔT:

$$\log\left(\frac{t_m}{t_0}\right) = \frac{1.18}{\beta} + \frac{(1-x)\theta}{2.303}\Delta T \tag{14}$$

where t_0 and t_m are intersections of the inflectional tangent with ordinates at one and zero in the 'normalized property'/log(t) plot, respectively. The expression $\log(t_m/t_0)$ is denoted as the stabilization period and is shown to be linearly dependent on the magnitude of the temperature jump ΔT under assumption of uniform T_0 for all down-jump relaxation curves. Furthermore, Málek [36] shows that both t_0 and t_m increase linearly with ΔT and the parameters $\Delta h^*/R$ and x can be evaluated from these dependencies according to:

$$\frac{\mathrm{d}\log(t_m)}{\mathrm{d}\Delta T} \cong \frac{\theta}{2.303} \tag{15}$$

$$\frac{\mathrm{d}\log(t_0)}{\mathrm{d}\Delta T} \cong \frac{x\theta}{2.303} \tag{16}$$

where $\Delta h^*/R$ can be evaluated from θ after by using Eq. (6). Eqs. (15) and (16) were derived assuming that the time required to reach the equilibrium state t_m is practically independent of the non-linearity effects due to the close proximity of the system to the equilibrium. On the other hand, the non-linearity effect greatly influences the time t_0 that characterizes the initial part of relaxation where the system starts to decrease linearly with log(t).

3. Experimental

3.1. Materials and methods

Polyvinyl acetate (PVAc) used in this study was the granular form of Mowillith 50 (molecular weight $M_w = 260\,000$). The volume relaxation measurements were performed using mercury dilatometry [38]. Preparation of the dilatometer, the measuring apparatus and several details of particular relaxation measurements were described in Ref. [39]. The constants characterizing proportions of our PVAc dilatometer (with similar meaning as in Ref. [39]) are $a = 84$ cm, $b = 18$ cm, $c_1 = 1.0$ cm, $c_2 = 0.7$ cm and the capillary diameter is 0.62 mm. Due to the relatively low heat

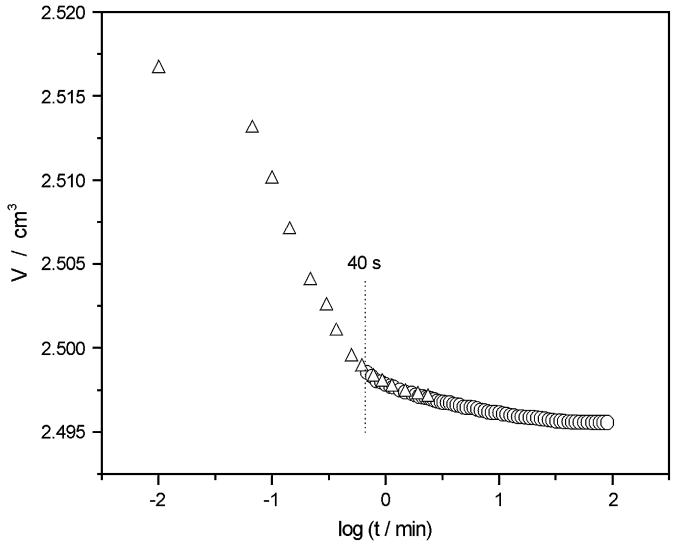

Fig. 2. Determination of the dilatometer time constant t_i from a down-jump experiment ($T_0 = 40$ °C, $T = 31$ °C). Triangles correspond to the very first readings immediately following the transfer of the dilatometer into the bath annealed at T. Circles correspond to the usually measured values when the first readings are taken after t_i.

conductivity of PVAc, the original granules were used directly as the sample instead of injection-moulding them into a thicker rod sample. The amount of dried PVAc granules batched into the dilatometer was 3.0 g and the mercury amount in the dilatometer was 50.5 g (this stands for the 0.7 PVAc/mercury volume ratio). The dilatometer sensitivity determined from the capillary length scale resolution was 1.18×10^{-5} cm^3/cm^3. Low sample/mercury ratio, thin wall of the sample holder and the very shape of the sample resulted in relatively low characteristic dilatometer time $t_i = 40$ s which was determined according to Ref. [39] (Fig. 2).

Enthalpy relaxation of PVAc was studied using the conventional DSC 822^e (Mettler, Toledo) equipped with refrigerated cooling accessory. Dry nitrogen was used as the purge gas at a rate of 20 cm^3/min. Melting temperatures of In, Zn and Ga were taken to calibrate the calorimeter, baseline was checked daily. During the sample preparation a thin layer of molten PVAc was spread on the bottom of standard aluminium pan to improve the thermal conduction and the pan was sealed afterwards. The mass of each batch was approximately 6 mg.

3.2. Thermal histories

Three types of experiments were performed during the volume relaxation measurements – non-isothermal determination of T_g at defined cooling rate, temperature down-jumps and the so-called "combined" experiments. The measurement of T_g was realized applying cooling rates 0.2 and 0.5 K min^{-1}. The dilatometer was annealed at 70 °C to assure that the sample is in equilibrium and then it was cooled to 5 °C. Actual temperature near by the dilatometer had to be recorded independently because a slight delay of the recorded versus programmed temperature was established. The cooling rate was verified this way too.

During down-jump experiments the dilatometer was first annealed at temperature T_0 for sufficiently long period of time to erase the previous thermal history and ensure that the sample is in equilibrium. The dilatometer was then manually transferred to the second bath and annealed at temperature T. The transfer was very quick and always done the same way. The first readings were taken after certain period of time (dilatometer time constant t_i) because of the distortion that would originate from the sample reaching the thermal equilibrium. The set of down-jump experiments with $T_0 = 35$ °C and T varying from 27 to 32 °C was performed in this study.

The combined experiment consists of down-jump from temperature T_0, annealing at temperature T_a for a certain period of time (annealing time t_a) followed by temperature up-jump to a temperature T ($T_a < T < T_0$). Time zero and first readings of mercury level were as in the case of the simple temperature jumps taken after the last temperature step (up-jump to T) after the time t_i needed for the sample to reach the thermal equilibrium. Two sets of combined experiments were performed: $T_0 = 40$ °C, $T = 31$ °C, annealing times t_a up to 24 h and $T_a = 10$ and 15 °C, respectively.

Enthalpic relaxation of PVAc was studied again through experiments with three different thermal histories. Individual experiments were already briefly described in the theoretical part, here they are denoted in order to distinguish them as: the classic cycles (three-step cyclic experiments described in Section 2.2), the intrinsic cycles (three-step cyclic experiments described at the end of Section 2.3) and the annealing experiments (four-step cyclic experiments described in Section 2.3). Exact temperature programs that were prepared for each type of thermal history are shown in Table 1. Each set of cyclic experiments was performed using the same sample which was kept in the measuring cell for the whole time in order to reduce the experimental error connected with slightly different positioning of the sample pan in the cell. The baseline was checked before and after each set of cycles. It was checked that no thermal degradation occurred in the sample by reproducing the first measurement in the set again at the end of the set.

3.3. Fitting procedure

The fitting program was created on the basis of TNM and AGS models. The input data were either in the form of the normalized relaxation function (isothermal experiments) or in the form of the normalized heat capacity (non-isothermal measurements) – Eqs. (17) and (18), respectively.

Table 1
Temperature programs for intrinsic cycles, classic cycles and annealing experiments

Step	Classic cycles	Intrinsic cycles	Annealing experiments
1	i 70/5	i 70/5	i 35/60
2	T −10/cooling q^-	T −10/cooling q^-	T 25/−40
3	T 70/10	T 70/heating q^+ ($q^+ = q^-$)	i 25/various t_a
4			T 70/10
Note	$q^- = 0.5, 1, 3, 5, 10, 15$	$q^- = 0.2, 0.5, 1, 2, 3, 5, 10, 15$	$t_a = 0, 0.1, 0.5, 1, 3, 5, 10, 15, 20, 30, 50, 100, 200, 300, 400, 600, 1100$

The programs are presented in the following pattern: non-isothermal steps are denoted with "T" followed by the temperature value [°C] the sample is cooled/heated to and after the slash is the appropriate cooling/heating rate [K min^{-1}]; the isothermal steps are denoted with "i" followed by annealing temperature [°C] and after the slash is annealing time [min].

$$\Phi(t) = \frac{T_f(t) - T}{T_0 - T} \tag{17}$$

$$C_p^N = \frac{dT_f}{dT} = \frac{C_p - C_{pg}}{C_{pl} - C_{pg}} \tag{18}$$

The fictive temperature is determined on the basis of the Boltzmann superposition integral over time that can be also replaced by a corresponding integral over temperature. In practice, the continuous cooling or heating is replaced by a sequence of n temperature jumps ΔT followed by isothermal holds with duration determined by the cooling and heating rates $\Delta t = \Delta T/q$ as suggested in Ref. [40]. The magnitude of ΔT must be sufficiently small to ensure linearity, $\Delta T = 1$ K was found to be satisfactory. The self-retarding kinetics can be introduced by dividing the aging time into k subintervals and calculating T_f and τ at the end of each. The subintervals are usually determined by dividing the aging time into even logarithmically spaced intervals. The fictive temperature can be calculated according to Eqs. (19) and (20) for non-isothermal and isothermal steps, respectively [40].

$$T_{f,n} = T_0 + \sum_{j=1}^{n} \Delta T_j \left\{ 1 - \exp\left[-\left(\sum_{k=j}^{n} \Delta T_k / Q_k \tau_k \right)^{\beta} \right] \right\} \tag{19}$$

$$T_{f,n} = T_0 + \sum_{j=1}^{n_A} \Delta T_j \left\{ 1 - \exp\left[-\left(\sum_{k=n_A}^{n} \Delta t_{e,k} / \tau_k \right)^{\beta} \right] \right\} \tag{20}$$

where T_0 is the initial equilibrium temperature and t_e is the annealing time.

The parameters of a given model were obtained through a non-linear optimization method by using the Levenberg–Marquardt algorithm. Minimum of the residual sum of squares (RSS) was sought in order to obtain the best fit. The input values of parameters are very important in order to obtain the absolute minimum of RSS and not only its local approximation. Therefore the non-fitting methods of obtaining these estimates are very important. Only that set of final values of the parameters which was reached using more different input estimates while having the lowest RSS could be taken as the correct one.

4. Results and discussion

4.1. Determination of T_g

Glass transition temperature is (as already mentioned above) dependent on the applied cooling or heating rate and, therefore, the T_g values obtained by various methods differ significantly. For this reason it is necessary to provide the information about the applied cooling/heating rate and the used method together with the value of T_g. In this work the glass transition temperature of PVAc was determined from volumetric and enthalpic measurements. The exact thermal histories are described in Section 3.2. The T_g measurement at the cooling rate 0.2 K min^{-1} is shown in Fig. 3. Glass transition temperature was evaluated as the intersection of extrapolated slopes of the curve in the range of glass and undercooled liquid, as indicated by the dashed line. For the case of capillary dilatometers, the evaluation of T_g is of course significantly affected by thermal lag between the malleablizing liquid and the sample. This was taken into account using correction based on the values of applied cooling rate and time constant of the dilatometer. Thermal expansion coefficients in glass α_g and in undercooled liquid α_l were

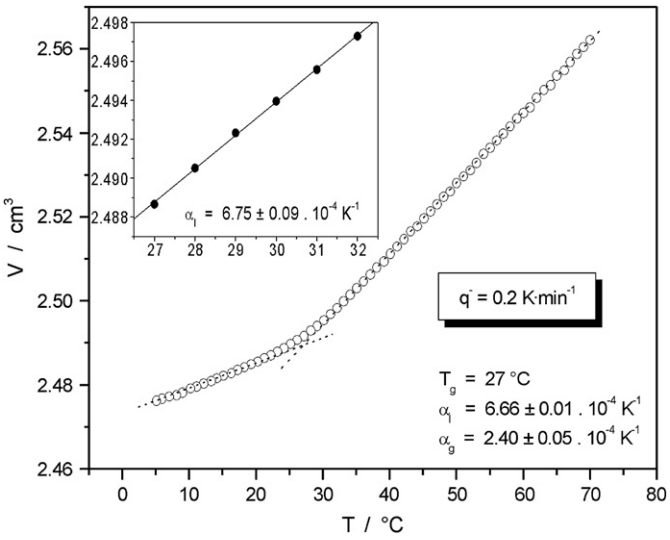

Fig. 3. Temperature dependence of PVAc volume measured dilatometrically at cooling rate $q^- = 0.2$ K min^{-1}. Evaluation of T_g is indicated by the dashed lines. The inset shows the dependence of equilibrium volume measured during isothermal down-jump experiments on the annealing temperatures.

determined from extrapolated slopes of the curve in appropriate regions according to the equation:

$$\alpha = \frac{1}{V}\left(\frac{dV}{dT}\right) \tag{21}$$

Evaluation of the similar measurement performed at cooling rate 0.5 K min^{-1} confirmed within experimental error these values. Furthermore, the value of α_l was evaluated from isothermal down-jump experiments – the equilibrium volumes for particular down-jumps were plotted against annealing temperatures as is shown in the inset in Fig. 3. This way determined value of α_l is within the experimental error equal with the values obtained from non-isothermal experiments. In addition, the absolute values of equilibrium volumes lie on the extrapolated liquid curve confirming the idea of the volume relaxing towards its equilibrium value represented by extrapolated liquid curve, this observation is generally accepted in respect of volume relaxation [6,11,41]. The value of enthalpic T_g taken from heating scans at 10 K min^{-1} performed in this work varied in the range 35–40 °C with respect to the previous thermal history. Difference in the heat capacity between the undercooled liquid and glassy state was found to be 0.50 ± 0.03 J g^{-1} K^{-1}. All values mentioned in this section are in a good agreement with those reported in literature [6,9,11,14,15].

4.2. TNM and AGS fits

Set of volumetric temperature down-jump experiments fitted with TNM model is depicted in Fig. 4 (sample volume was converted into the fictive temperature). The same experimental data were also fitted using the AGS model, the quality of the fit was equal to that by TNM model. For both models a single set of parameters was used to fit all the corresponding (volume or enthalpy) data presented in this work. The values of TNM and AGS parameters are summarized in Table 2. As can be seen in Fig. 4, the "initial" fictive temperature of the measurement decreases together with the annealing temperature T (assuming constant T_0). Furthermore, it can be easily calculated that the amount of information lost during the thermal stabilization of the sample (time constant t_i) also decreases with decreasing T (48% lost during stabilization at 32 °C, 36% lost at 27 °C). These down-jump effects are commonly

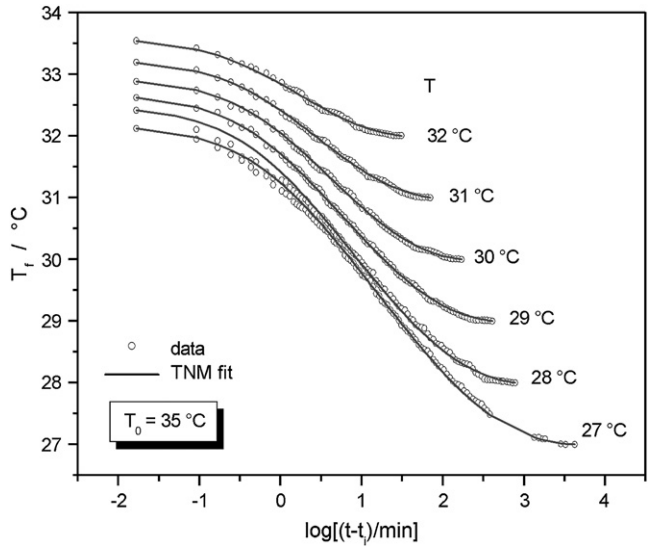

Fig. 4. Set of temperature down-jump experiments ($T_0 = 35$ °C, T marked in the figure). The experimental data are fitted using TNM model – the parameters are listed in Table 2.

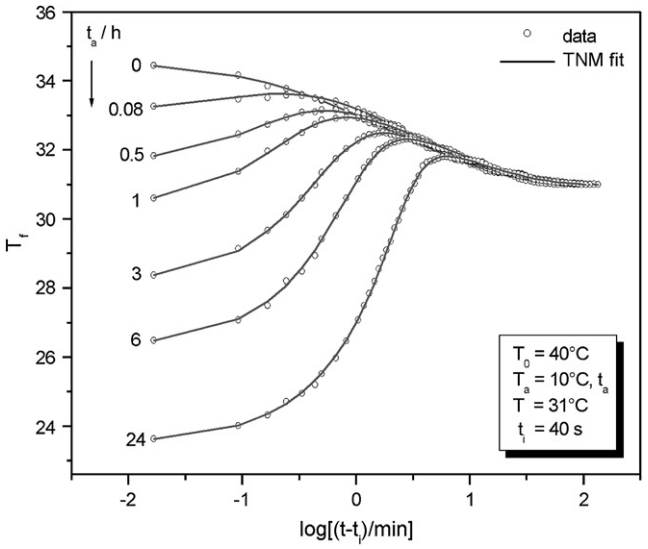

Fig. 5. Set of combined dilatometric experiments ($T_0 = 40$ °C, $T_a = 10$ °C, $T = 31$ °C, annealing times t_a are marked in the figure). The experimental data are fitted using TNM model – the parameters are listed in Table 2.

observed when dealing with methods that require some thermal stabilization of the sample and are caused due to the relaxation process proceeding at different thermal gradients (which in addition change during the stabilization). This part of thermal history was of course involved in the fitting process too, more about t_i and thermal gradient in mercury dilatometry can be found in Ref. [39].

Nevertheless, the large amount of information lost during down-jump experiments together with the fact that these experiments are relatively easy to fit with a wide variety of parameters led us to perform experiments with more complex thermal history to determine the parameters of the models more accurately. For this reason two sets of combined experiments were performed, exact thermal histories together with further details of these experiments are introduced in Section 3.2. These two sets of combined experiments with T_a equal to 10 and 15 °C are shown in Figs. 5 and 6, respectively. The combined experiments provide several advantages for the fitting process compared to simple temperature jumps. Thermal history that consists of two consecutive temperature jumps where the sample during the first jump did not reach equilibrium structure for that temperature provides due to the distribution of relaxation times an extreme on the isotherm following the second jump. This is very advantageous for the fitting process as each such curve can be fitted only within exact narrow combination of parameters. Second advantage of combined experiments lies in lower amount of information lost during the stabilization period t_i. The structure of the sample becomes very compact during annealing at a low temperature T_a so it lasts much longer for it to start to change rapidly during the following heating step and stabilization period t_i. This leads to much lower amounts of relaxation information lost – e.g. 13% lost for 12 h long annealing at 15 °C. In addition, time required for the very measurement (several hours to reach equilibrium at 31 °C) is incomparable to that for down-jumps included in the previously described set (days to weeks or months). Shorter measurement time also results in an increased accuracy of the measurement due to the unnecessity of keeping all experiment conditions invariable. Volumetric values of TNM and AGS parameters (Table 2) were in fact determined on the basis of fitting the experimental data depicted in Figs. 5 and 6, temperature down-jumps were then fitted with the same set of parameters to verify the values.

In order to obtain TNM and AGS parameters for enthalpic relaxation several sets of classic and intrinsic cycles (see Section 3.2) were fitted using the appropriate models. Several examples of classic cycle curves are shown in Fig. 7, the heat capacity had to be normalized for the purposes of consequential fitting. As can be seen, TNM model provides relatively accurate description of the experimental data. AGS model provided a slightly worse but still well acceptable fit within relatively wide variety of parameter combinations. The essential value was that of parameter B, with this parameter held constant anywhere in the range 6.5–8.5 kK equally good fits were obtained. Moreover, the parameter B tended to decrease to unrealistic values for certain curves. Values of parameters for both models are summarized in Table 2, set of AGS values was chosen for $B = 8.2$ kK (taken from volumetric measurements).

One of the aims of this paper was to compare volume and enthalpy relaxation on the basis of TNM or AGS description. Comparing the volume and enthalpy relaxation described by TNM model one can see that the apparent activation energy $\Delta h^*/R$ and pre-exponential factor A are similar for both while the non-linearity parameter x and non-exponentiality parameter β are both notably higher in the case of enthalpy relaxation. Similar observation was made previously for volume and enthalpy relaxation of amorphous selenium [42], the reported increase in parameters x and β was by an analogous amount as here in the case of PVAc. Similar relation between volumetric TNM and AGS parameters was

Table 2
Values of the TNM and AGS parameters obtained by the best fit of enthalpy and volume relaxation data

	TNM model				AGS model			
	$\Delta h^*/R$ (kK)	lnA (s)	x (–)	β (–)	B (kK)	lnA (s)	T_2 (K)	β (–)
Volume	55.6 ± 0.5	−177.5 ± 1.5	0.32 ± 0.05	0.46 ± 0.05	8.2 ± 0.2	−59 ± 3	174 ± 10	0.46 ± 0.05
Enthalpy	55.6 ± 0.5	−177.5 ± 1.5	0.43 ± 0.05	0.50 ± 0.05	8.2*	−70 ± 2	195 ± 4	0.47 ± 0.02

For detailed description of * see the text.

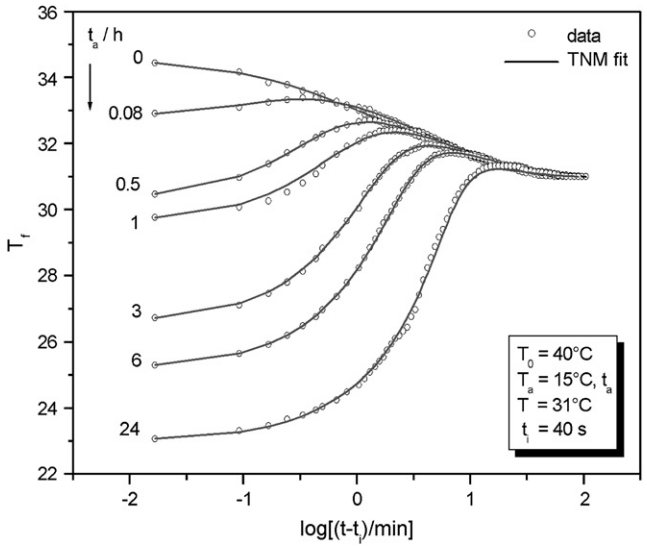

Fig. 6. Set of combined dilatometric experiments ($T_0 = 40\,^{\circ}C$, $T_a = 15\,^{\circ}C$, $T = 31\,^{\circ}C$, annealing times t_a are marked in the figure). The experimental data are fitted using TNM model – the parameters are listed in Table 2.

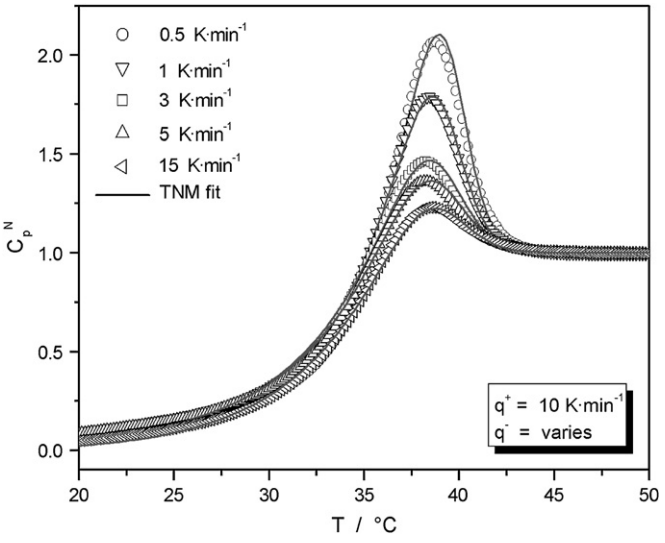

Fig. 7. Best fits of the normalized heat capacity C_p^N curves from enthalpic classic cycles performed at heating rate 10 K min^{-1} following a cooling step at various cooling rates. The experimental data are fitted using TNM model – the parameters are listed in Table 2.

in the case of amorphous selenium also noticed [43] – the same value of β for both models, T_2 being close to the Kauzmann temperature T_K and a similar ratio of $\Delta h^*/B$ for a-Se and PVAc.

In the following text several non-fitting methods of TNM parameters' evaluation will be presented. The parameters obtained through this way can either serve as the first input values in the fitting process or can confirm its final results.

4.3. Comparison to the data of Kovacs

Kovacs published in his famous work [6] quite an amount of precise experimental relaxation data on PVAc. The experiments that Kovacs performed cover all basic types of experiments – including down-jump, up-jump and combined measurements. From certain point of view, several experiments have somewhat extreme thermal history, e.g., the combined experiment shown in Fig. 9 of Ref. [6] where the annealing time at $T_a = 25\,^{\circ}C$ is $t_a \sim 1500$ h. Nevertheless, in order to compare our volume measurements with literature we have digitized all the PVAc volumetric data reported by Kovacs in Ref. [6] and fitted them using the TNM model. All the down-jump, up-jump and combined experiments were fitted using the same set of parameters as was that for our volumetric data (except for the logarithm of the pre-exponential factor A that for the data of Kovacs varied in the range $\ln A = -175 \pm 2$) providing a reasonably good fit. The quality of the fit of course varied depending on the particular thermal history as the down-jump and up-jump experiments can be fitted much more easily compared to the combined experiments. The quality is also significantly influenced by the fact that although Kovacs reports for his data the value of characteristic dilatometer time $t_i = 36$ s we cannot be absolutely sure about this value. The characteristic time of the dilatometer can be determined by a number of ways where each method provides slightly different value of t_i. Description of the fitted thermal history is partially based on the dilatometer time t_i and its wrong value can lead to the deformation of the fit. According to our simulations in either way wrong value of t_i (too high or too low) provides for certain thermal histories a plateau on the measured data during the initial phase of the measurement. This plateau cannot be fitted within the range of TNM parameters used for the rest of measurements. More about characteristic time of the dilatometer t_i, its determination and origin of the above-mentioned plateau can be found in Ref. [39,43]. Example of the reproduced combined experiments made by Kovacs [6, Fig. 24, p 480] fitted using TNM model and volume parameters given in Table 2 (except for the logarithm of pre-exponential factor $\ln A$ that equals -175 ± 2) is shown in Fig. 8. Example of simple down-jump experiments made by Kovacs [6, Fig. 15, p. 465] fitted using TNM model and again the same parameters is shown in Fig. 9. For more detailed information about the experiments see the figure captions.

4.4. Estimates of $\Delta h^*/R$

In this chapter, three ways of $\Delta h^*/R$ estimation will be applied – inflectional analysis as an alternative method for volumetric data,

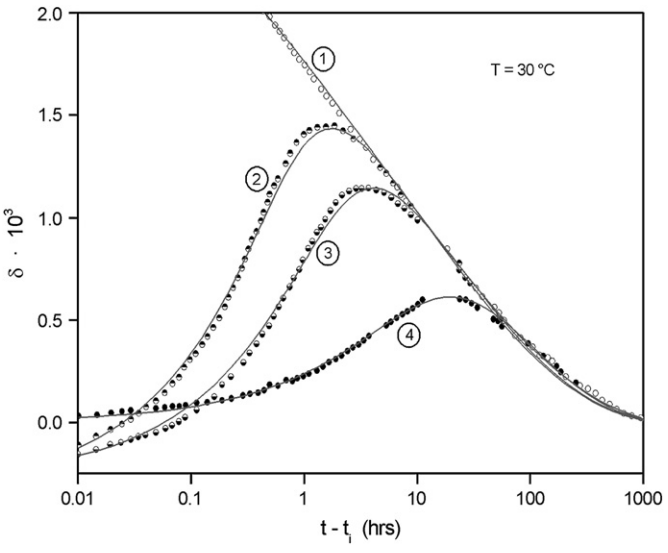

Fig. 8. Reproduced data of Kovacs taken from Ref. [6, Fig. 24, p 480]. Curve no. 1 corresponds to the down-jump experiment ($T_0 = 40\,^{\circ}C$, $T = 30\,^{\circ}C$), other three curves are combined measurements with $T_0 = 40\,^{\circ}C$ and $T = 30\,^{\circ}C$ which differ by the annealing temperature and time. Curve no. 2 corresponds to $T_a = 10\,^{\circ}C$ and $t_a = 160$ h, curve no. 3 corresponds to $T_a = 15\,^{\circ}C$ and $t_a = 140$ h, curve no. 4 corresponds to $T_a = 25\,^{\circ}C$ and $t_a = 90$ h. Solid lines correspond to the TNM fit. TNM parameters correspond to those evaluated from our data (listed in Table 2) except for $\ln A = -175 \pm 2$.

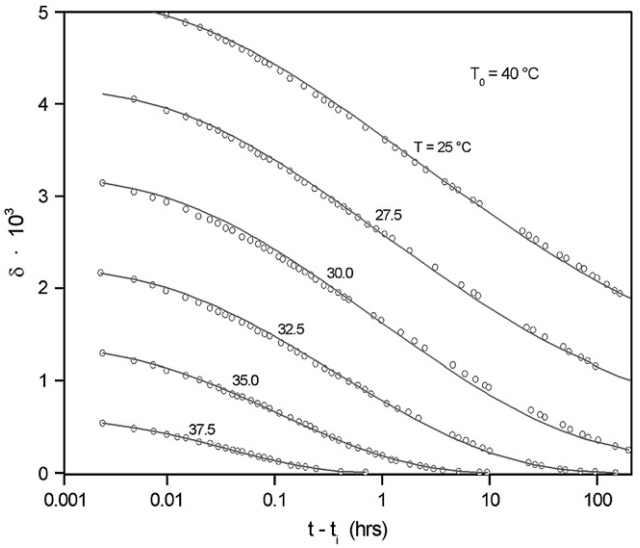

Fig. 9. Reproduced data of Kovacs taken from Ref. [6, Fig. 15, p 465]. Experimental data correspond to various down-jump experiments ($T_0 = 40$ °C, T varies). Solid lines correspond to the TNM fit. TNM parameters correspond to those evaluated from our data (listed in Table 2) except for $\ln A = -175 \pm 2$.

evaluation from classic and intrinsic cycles for enthalpy measurements.

Inflectional analysis proposed by Málek [36] and described in Section 2.4 is a simple but effective method for determining certain TNM parameters from a set of temperature down-jump experiments. Unfortunately a lot of experimental techniques suffer from needing some kind of temperature stabilization prior to any isotherm that is following a temperature change. Due to this stabilization, the initial time t_0 of the isothermal relaxation is uncertain and can be determined only with large error. The only parameter that is independent of t_0 is the effective activation energy $\Delta h^*/R$. This parameter can be evaluated (Eq. (15)) only by use of equilibrium times t_m which can be determined accurately. The analysis of down-jump volumetric experiments performed in this work is displayed in Fig. 10. The value of $T_g = 27$ °C used to convert Kovacs's θ to $\Delta h^*/R$ was taken from non-isothermal measurements. Apparent activation energy $\Delta h^*/R$ was then calculated to be 58 kK. The true value of T_g would in case of the mentioned down-jumps (taking into account thermal history) probably be 35 °C or near this temperature – applying this value to the conversion of θ gives $\Delta h^*/R$ about 3 kK higher than for $T_g = 27$ °C.

Second method of $\Delta h^*/R$ estimation is based on Eq. (13) applied to the DSC intrinsic cycles (theory described in Section 2.3, exact thermal history is given in Table 1). Three sets of intrinsic cycles were performed in order to obtain average value of T_p for each cooling rate. Linear fit to the data plotted as a logarithm of cooling rate versus maximum of the relaxation peak is shown in Fig. 11. The slope of this dependence gives $\Delta h^*/R = 55$ kK. It can be seen that the error of this measurement is very low as the maximum of the peak can be determined very accurately and any slight changes of experimental conditions that can influence the baseline or thermal gradients in the sample do not shift the value of T_p. It was further confirmed by several other performed intrinsic cycle sets that the value of T_p is for the given cooling and heating rate independent of the concrete temperatures the sample was cooled from and to.

Finally, $\Delta h^*/R$ can be estimated from the dependence of T_g on cooling rate (Section 2.2). Three sets of classic DSC cycles with thermal history given in Table 1 were performed, the fictive temperature reached during the cooling step was determined by the equal area method according to Eq. (5). Logarithm of cooling rate versus reciprocal fictive temperature is plotted in Fig. 12. Linear fit to these data yields a slope that gives $\Delta h^*/R = 91$ kK. Errors displayed in Fig. 12 are much higher than those of T_p measured during intrinsic cycles (Fig. 11). This is simply caused by the fact that fictive temperature is evaluated from the whole area under the experimental curve and even slight changes in height or width of the relaxation peak influence the resulting integral area significantly.

To summarize this section one can say that the analysis of volumetric data proposed by Málek [36] together with the evaluation from intrinsic DSC cycles give values of the activation energy of structural relaxation $\Delta h^*/R$ close to that determined from curve fitting. On the other hand, the value of $\Delta h^*/R$ determined from classic cycles according to Eq. (4) is exceedingly high compared to the value from curve fitting, similar observation was made previously for amorphous selenium [42] and can also be derived from results of Zumailan [44], Cortés et al. [45] and Echeverría et al. [46]. Values of $\Delta h^*/R$ reported for PVAc in literature include the following: 96.7 kK determined from classic cycles by Hutchinson and Kumar [14], 88 kK determined from curve fitting of several enthalpic cycles and annealing experiments performed by Hodge

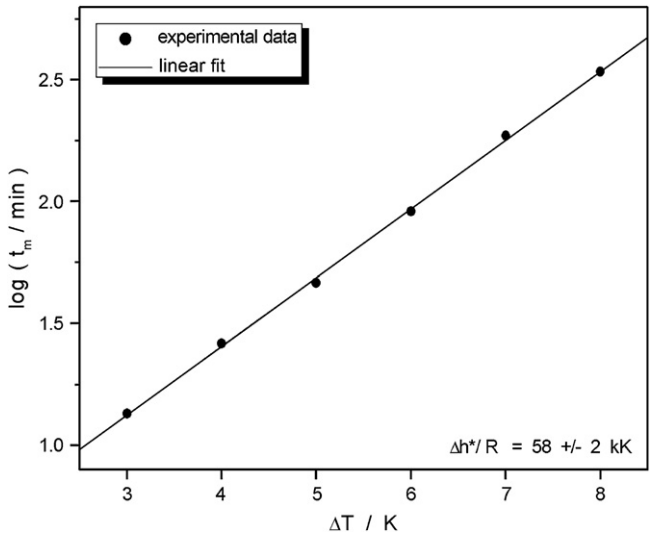

Fig. 10. Logarithm of the equilibrium time t_m as a function of the magnitude of dilatometric down-jump experiment $\Delta T = T_0 \times T$. Linear fit of the data was applied in compliance with Eq. (15).

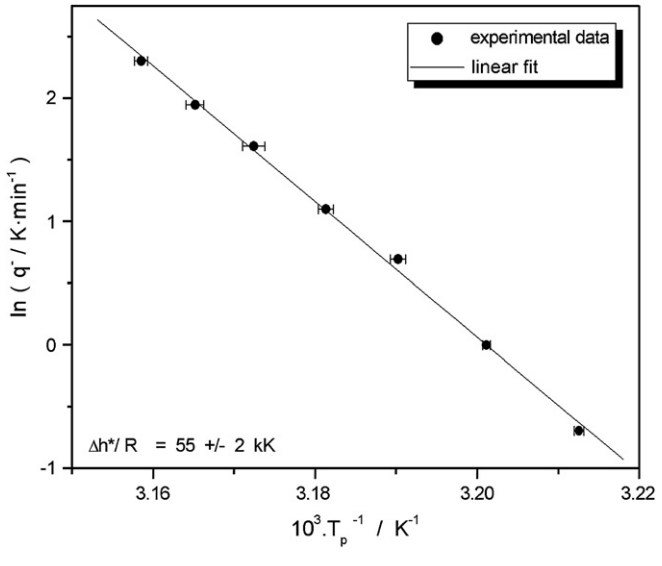

Fig. 11. Estimation of the apparent activation energy of structural relaxation $\Delta h^*/R$ from enthalpic intrinsic cycles. Each experimental point is taken as a mean value of three measurements – linear fit of the data was applied in compliance with Eq. (13).

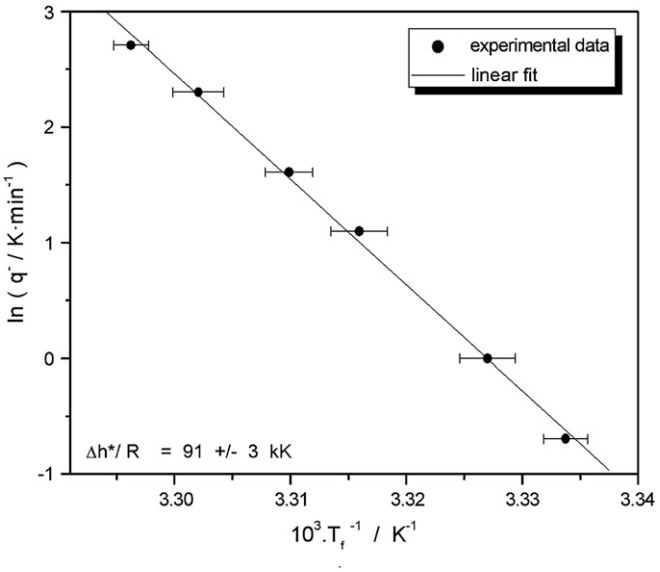

Fig. 12. Estimation of the apparent activation energy of structural relaxation $\Delta h^*/R$ from enthalpic classic cycles. Each experimental point is taken as a mean value of three measurements – linear fit of the data was applied in compliance with Eq. (4).

[16] (quality of the fits is slightly questionable), 71 kK determined from fits of enthalpic measurements by Sasabe and Moynihan [15] and 30.7 kK calculated by Hutchinson and Kumar [14] from data presented by Cowie et al. [47] – this large discrepancy is according to Ref. [14] caused by the fact that Cowie et al. fitted the experimental data with their semi-empirical CF function that is based on the KWW function but not taking into account that the relaxation time depends on the structure of the glass.

4.5. Estimates of β and x

Estimation of non-linearity parameter x can be made on the basis of peak-shift method according to Eqs. (9) and (12). Fig. 13 shows the dependence of the relaxation peak maximum T_p on excess enthalpy δ_H for annealing experiments described in Section 3.2. Annealing temperature was chosen to be 25 °C (about 15 °C below enthalpic T_g measured at 10 K min^{-1}) which was low enough for the sample not to reach equilibrium state within the given timescale. Annealing times ranged from 0.5 to 1100 min, longer annealing times could not be applied due to the technique limitation. Short annealing times were applied in order to show the occurrence of upper peaks during experiments where only low amount of annealing is applied. This can be seen in Fig. 13 where main peaks started to occur for annealing times longer than approximately 3 h. Slope of the dependence for the main peaks is indicated by the full line in the figure. Parameter $x = 0.48 \pm 0.04$ was evaluated from this slope ($\Delta C_p = 0.50$ J g^{-1} K^{-1} was taken for the calculation). However, it can be argued whether the slope presented for our data would not increase more with measurements performed for annealing times longer than 1100 min (which would result in lower value of x).

Parameters x and β can be further evaluated from the classic cycles where experimental data are compared to the simulation of the dependence of the normalized relaxation peak height C_p^{max} on logarithm of the ratio of cooling rate to heating rate. Theoretical curves for several combinations of x and β together with experimental PVAc data obtained from classic cycles are depicted in Fig. 14 (see figure captions for details), values of the apparent activation energy $\Delta h^*/R$ and of the pre-exponential factor A were taken from the curve-fitting results to calculate the theoretical curves. The general trend of decreasing C_p^{max} with increasing $\log(|q^-|/q^+)$ is common to all of these theoretical curves. Comparison of experimental data with theoretical curves provides an estimate of the range within which the particular parameters can be localized. Only a rough estimate can be made in case of both parameters being evaluated as curves for multiple combinations may fit the experimental data. On the other hand, if parameter x is already known from, e.g., peak-shift method, range for parameter β can be easily determined.

Both methods presented in this section provide accurate and meaningful results but careful analysis of the data has to be applied. In the case of peak-shift method only sufficiently long annealing times have to be taken into account (until the slope of linear trend between T_p and δ_H can be reliably determined). In the case of the classic cycle simulation the values of $\Delta h^*/R$ and pre-exponential factor A (and preferably also the value of x) have to be known prior to estimation of any other parameters. Values of non-linearity and non-exponentiality parameters estimated in this chapter are in a rather good agreement with values obtained from curve fitting

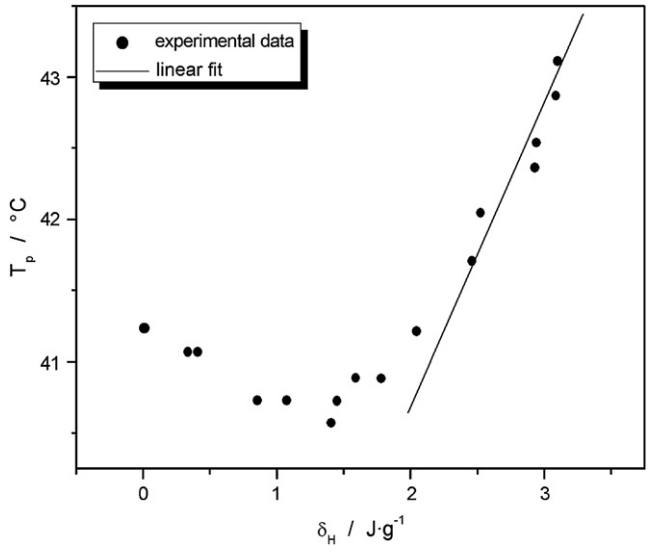

Fig. 13. Dependence of the maximum of the relaxation peak T_p on enthalpy loss δ_H during annealing of PVAc at 25 °C following cooling at 40 K min^{-1} from equilibrium at 35 °C. Linear fit of the data was applied in compliance with Eq. (9).

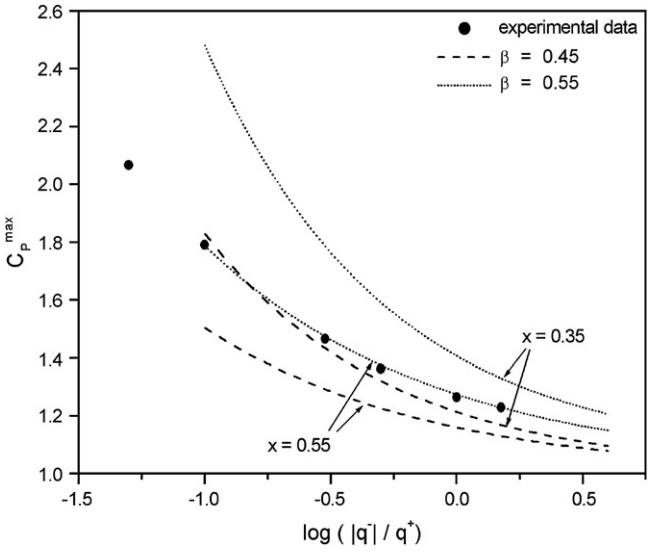

Fig. 14. Dependence of the normalized relaxation peak height C_p^{max} on $\log(|q^-|/q^+)$ for classic enthalpic cycles. The theoretical curves were calculated for $\beta = 0.45$ (dashed line) and $\beta = 0.55$ (dotted line), each with two different values of x (0.35 and 0.55).

(Table 2). However, curve fitting gives better results for these two parameters compared to values reported in literature. Hodge [16] reports values $x = 0.27$ and $\beta = 0.51$ from curve fitting of various cycle and annealing experiments, and enthalpy relaxation parameters obtained by Moynihan and Sasabe [15] also from curve fitting are $x = 0.41$ and $\beta = 0.51$. Hutchinson [14] reports $x = 0.44$ from the peak-shift method (annealing times up to 2000 h!) and $0.456 \leq \beta \leq 0.6$ from the comparison of simulated and experimental classic cycles. Cowie et al. [47] reports somewhat lower value of non-exponentiality parameter $0.33 \leq \beta \leq 0.45$ which is probably caused by omitting the non-linearity from their CF equation as stated in Ref. [14].

5. Conclusions

Structural relaxation of polyvinyl acetate was studied using mercury dilatometry and differential scanning calorimetry. The models of Tool–Narayanaswamy–Moynihan and Adam–Gibbs–Scherer were used to describe numerous volumetric and enthalpic measurements. Single set of volume and enthalpy relaxation parameters for each model was determined and used to fit all the performed experiments. Comparison of the volume and enthalpy relaxation was made on the basis of TNM model parameters suggesting that the apparent activation energy $\Delta h^*/R$ and the pre-exponential factor A are the same for both types of relaxation while the non-linear and non-exponential behaviors are slightly weaker in the case of enthalpy relaxation. This result surprisingly well agrees with our previous measurements on amorphous selenium. In addition, several methods of TNM parameters' estimation were tested on our data. Estimation of $\Delta h^*/R$ was performed following three different methods – inflectional analysis, evaluation from intrinsic cycles and evaluation from classic cycles. A good agreement between estimates and curve-fitting results was achieved. Only the last-mentioned evaluation from classic cycles provided a value that was inconsistent with results from curve fitting which is, however, in the case of this method an occasionally observed issue. Furthermore, the peak-shift method and the simulation method have been applied on the enthalpy relaxation data in order to estimate parameters x and β. Both methods provided results that were in a relatively good agreement with values obtained by curve fitting.

Acknowledgements

The financial support of the Czech Ministry of Education, Youth and Sports, research project MSM 0021627501 is gratefully acknowledged.

References

[1] Debenedetti PG, Stillinger FH. Nature 2001;410:259–67.
[2] Scherer GW. Relaxation in glass and composites. New York: John Wiley & Sons; 1986 [chapter 9].
[3] Struik LCE. Physical aging of amorphous polymers and other materials. New York: Elsevier; 1978.
[4] Hodge IM. J Non-Cryst Solids 1994;169:211–66.
[5] Angell CA, Ngai KL, McKenna GB, McMillan PF, Martin SW. J Appl Phys 2000; 88(6):3113–57.
[6] Kovacs AJ. Fortschr Hochpolym Forsch 1963;3:394–507.
[7] Struik LCE. Polymer 1997;38:5233–41.
[8] McKenna GB, Vangel MG, Rukhin AL, Leigh SD, Lotz B, Straupe C. Polymer 1999;40:5183–205.
[9] Donth E, Hempel E. J Non-Cryst Solids 2002;306(1):76–89.
[10] Aharoune A, Marceron-Balland P, Cunat C. Mech Time-Depend Mater 2001; 5(4):345–77.
[11] Delin M, Rychwalski RW, Kubát J, Klason C, Hutchinson JM. Polym Eng Sci 1996;36(24):2955–67.
[12] Cowie JMG, Harris S, McEwen IJ. Macromolecules 1998;31(8):2611–5.
[13] McKinney JE, Goldstein M. J Res Natl Bur Stand 1974;A78(3):331–53.
[14] Hutchinson JM, Kumar P. Thermochim Acta 2002;391(1–2):197–217.
[15] Sasabe H, Moynihan CT. J Polym Sci 1978;16(8):1447–57.
[16] Hodge IM. Macromolecules 1987;20(11):2897–908.
[17] Donth E, Korus J, Hempel E, Beiner M. Thermochim Acta 1997;305:239–49.
[18] Cowie JMG, Ferguson R, Harris S, McEwen IJ. Polymer 1998;39(18):4393–7.
[19] Kubát MJ, Vernel J, Rychwalski RW, Kubát J. Polym Eng Sci 1998;38(8):1261–9.
[20] Tribone JJ, O'Reilly JM, Greener J. Macromolecules 1986;19(6):1732–9.
[21] Gardon R, Narayanaswamy OS. J Am Ceram Soc 1970;53(7):380–5.
[22] Tool AQ. J Am Ceram Soc 1946;29(9):240–53.
[23] Narayanaswamy OS. J Am Ceram Soc 1971;54(10):491–8.
[24] Moynihan CT, Easteal AJ, DeBolt MA, Tucker J. J Am Ceram Soc 1976;59(1–2): 12–6.
[25] Scherer GW. J Am Ceram Soc 1984;67(7):504–11.
[26] Scherer GW. J Am Ceram Soc 1986;69(5):374–81.
[27] Hodge IM. Macromolecules 1986;19(3):936–8.
[28] Hodge IM. J Non-Cryst Solids 1991;131:435–41.
[29] Ritland HN. J Am Ceram Soc 1955;38(2):86–8.
[30] DeBolt MA, Easteal AJ, Macedo PB, Moynihan CT. J Am Ceram Soc 1976; 59(1–2):16–21.
[31] Hutchinson JM, Ruddy M. J Polym Sci B 1990;28(11):2127–63.
[32] Hutchinson JM, Kovacs AJ. Polym Eng Sci 1984;24(14):1087–103.
[33] Hutchinson JM, Ruddy M. J Polym Sci B 1988;26(11):2341–66.
[34] Kovacs AJ, Aklonis JJ, Hutchinson JM, Ramos AR. J Polym Sci B 1979;17(7): 1097–162.
[35] Ramos AR, Hutchinson JM, Kovacs AJ. J Polym Sci B 1984;22(9):1655–96.
[36] Málek J. Thermochim Acta 1998;313:181–90.
[37] Málek J, Montserrat S. Thermochim Acta 1998;313:191–200.
[38] ASTM D 864; 1952.
[39] Svoboda R, Pustková P, Málek J. J Non-Cryst Solids 2006;352:4793–9.
[40] Hodge IM, Berens AR. Macromolecules 1982;15(3):762–70.
[41] Hutchinson JM. The physics of glassy polymers. London: Chapman & Hall; 1997.
[42] Svoboda R, Pustková P, Málek J. J Phys Chem Solids 2007;68:850–4.
[43] Málek J, Svoboda R, Pustková P, Cicmanec P. J Mater Res, in press.
[44] Zumailan A. Mater Lett 2002;57(1):94–8.
[45] Cortés P, Montserrat S, Ledru J, Saiter JM. J Non-Cryst Solids 1998;235: 522–6.
[46] Echeverría I, Kolek PL, Plazek DJ, Simon Sl. J Non-Cryst Solids 2003;324(3): 242–55.
[47] Cowie JMG, Harris S, McEwen IJ. J Polym Sci B 1997;35(7):1107–16.